

ORIGINAL ARTICLE

Dietary calcium regulates ROS production in aP2-agouti transgenic mice on high-fat/high-sucrose diets

X Sun and MB Zemel

Department of Nutrition, University of Tennessee, Knoxville, TN, USA

Objective: We have previously demonstrated that $1\alpha, 25(\text{OH})_2\text{D}_3$ promotes adipocyte reactive oxygen species (ROS) production. We have now evaluated whether decreasing $1\alpha, 25(\text{OH})_2\text{D}_3$ levels by increasing dietary calcium will decrease oxidative stress *in vivo*.

Methods: We fed low-calcium (0.4% Ca) and high-calcium (1.2% Ca from CaCO_3) obesity-promoting (high sucrose/high fat) diets to aP2-agouti transgenic mice and assessed regulation of ROS production in adipose tissue and skeletal muscle.

Results: Mice on the high-calcium diet gained 50% of the body weight ($P=0.04$) and fat ($P<0.001$) as mice on the low-calcium diet (0.4% Ca). The high-calcium diet significantly reduced adipose intracellular ROS production by 64 and 18% ($P<0.001$) and inhibited adipose tissue nicotinamide adenine dinucleotide phosphate oxidase expression by 49% ($P=0.012$) and 63% ($P=0.05$) in visceral and subcutaneous adipose tissue, respectively. Adipocyte intracellular calcium ($[\text{Ca}^{2+}]_i$) levels were suppressed in mice on the high-calcium diet by 73–80% ($P<0.001$). The high-calcium diet also induced 367 and 191% increases in adipose mitochondrial uncoupling protein 2 (UCP2) expression ($P<0.001$) in visceral and subcutaneous adipose tissue, respectively. The pattern of UCP3 expression and indices of ROS production in skeletal muscle were consistent with those in adipose tissue. The high-calcium diet also suppressed 11β -hydroxysteroid dehydrogenase (11β -HSD) expression in visceral adipose tissue by 39% ($P=0.034$). 11β -HSD expression was markedly higher in visceral vs subcutaneous adipose tissue in mice on the low-calcium diet ($P=0.034$), whereas no difference was observed between the fat depots in mice on the high-calcium diet.

Conclusion: These data support a potential role for dietary calcium in the regulation of obesity-induced oxidative stress.

International Journal of Obesity advance online publication, 7 March 2006; doi:10.1038/sj.ijo.0803294

Keywords: ROS; calcium; UCP2; UCP3; $1\alpha, 25(\text{OH})_2\text{D}_3$

Introduction

Reactive oxygen species (ROS) production is increased in obesity and diabetes.^{1–4} It has been postulated that hyperglycemia and hyperlipidemia, key clinical manifestations of obesity and diabetes, may promote ROS production through multiple pathways.^{5–7} Previous studies from this laboratory demonstrate an anti-obesity effect of dietary calcium, with increasing dietary calcium inhibiting lipogenesis, stimulating lipolysis and thermogenesis and increasing adipocyte apoptosis.^{8–9} These effects are mediated by suppression of $1\alpha, 25(\text{OH})_2\text{D}_3$ -induced stimulation of Ca^{2+} influx and inhibition of adipocyte UCP2 gene expression.^{10,11} We have also

recently shown that ROS production is modulated by mitochondrial uncoupling status and cytosol calcium signaling, and that $1\alpha, 25(\text{OH})_2\text{D}_3$ regulates ROS production in cultured murine and human adipocytes.¹² Accordingly, we propose that $1\alpha, 25(\text{OH})_2\text{D}_3$ may regulate oxidative stress in adipocytes by promoting ROS production, and that modulating $1\alpha, 25(\text{OH})_2\text{D}_3$ through dietary calcium may affect oxidative stress *in vivo*. Accordingly, we have now investigated the effect of dietary calcium on ROS production and the potential underlying mechanisms in adipose tissue and skeletal muscle in an animal obesity model.

aP2-agouti transgenic mice were used as a model of obesity-induced oxidative stress. We previously described these mice as useful models for diet-induced obesity in a genetically susceptible human population in that they are not obese on a standard AIN-93 G diet, but develop mild to moderate obesity and hyperglycemia when fed high-sucrose and/or high-fat diets,^{13,14} indicating that aP2-agouti transgenic mice may be a potential animal model to study obesity-associated oxidative stress. Accordingly, before the dietary

Correspondence: Dr MB Zemel, Department of Nutrition, University of Tennessee, 1215 West Cumberland Avenue, #229, Knoxville, TN 37996-1900, USA.

E-mail: mzemel@utk.edu

Received 20 September 2005; revised 9 January 2006; accepted 1 February 2006

calcium experiments, we compared adipose ROS production between aP2 transgenic mice and wild-type mice following short-term exposure to the high-fat-high-sucrose diet in order to verify its suitability as an animal model.

Materials and methods

Animals and diets

Animal pilot study. Six-week-old male aP2-*agouti* transgenic mice and wild-type male littermates ($n = 12/\text{group}$) from our colony were utilized. Six mice randomly selected from each group were killed to provide baseline data and the remaining six mice in each group were put on a modified AIN 93 G diet¹⁵ with sucrose as the sole carbohydrate source and providing 64% of energy, and fat increased to 25% of energy with lard as previously described.^{13,14} Mice were studied for 9 days, during which food intake and spillage were measured daily and body weight, fasting blood glucose and food consumption assessed weekly. At the conclusion of the study, all mice were killed under isoflurane anesthesia and fat pads were immediately excised, weighed and used for further study, as described below.

Diet study. At 6 weeks of age, 20 male aP2-*agouti* transgenic mice from our colony were randomly divided into two groups (10 mice/group) and fed a modified AIN 93 G diet with suboptimal calcium (calcium carbonate, 0.4%) or high calcium (calcium carbonate, 1.2%), respectively, with sucrose as the sole carbohydrate source and providing 64% of energy, and fat increased to 25% of energy with lard. Mice were studied for 3 weeks, during which food intake and spillage were measured daily and body weight, fasting blood glucose and food consumption assessed weekly. At the conclusion of the study, all mice were killed under isoflurane anesthesia and blood collected via cardiac puncture; visceral fat pads (perirenal and abdominal), subcutaneous fat pads (subscapular) and soleus muscle were immediately excised, weighed and used for further study, as described below.

This study was approved from an ethical standpoint by the Institutional Care and Use Committee of The University of Tennessee.

Measurement of adipocyte intracellular Ca^{2+}

Adipose tissue was first washed several times with Hank's balanced salt solution (HBSS), minced into small pieces and digested with 0.8 mg/ml type I collagenase in a shaking water bath at 37°C for 30 min. Adipocytes were then filtered through sterile 500- μm nylon mesh and cultured in Dulbecco's modified Eagle's medium (DMEM) supplemented with 1% fetal bovine serum (FBS). Cells were cultured in suspension and maintained in a thin layer at the top of culture media for 2 h for cell recovery. Intracellular calcium $[\text{Ca}^{2+}]_i$ in isolated mouse adipocytes was measured by using a fura-2 dual wavelength fluorescence imaging system.

Before $[\text{Ca}^{2+}]_i$ measurement, adipocytes were incubated in serum-free medium for 2 h and rinsed with HBSS containing the following components (in mmol/l): NaCl 138, CaCl_2 1.8, MgSO_4 0.8, NaH_2PO_4 0.9, NaHCO_3 4, glucose 5, glutamine 6 Hepes 20 and bovine serum albumin 1%. Adipocytes were loaded with fura-2 acetoxymethyl ester (AM) (10 $\mu\text{mol/l}$) in the same buffer in dark for 1 h at 37°C. Adipocytes were rinsed with HBSS three times to remove extracellular dye and then incubated at room temperature for an additional 30 min to permit complete hydrolysis of cytoplasmic fura-2 AM. A thin layer of adipocytes was plated in 35 mm dishes with glass coverslips (P35G-0-14-C, MatTek Corporation, Ashland, MA, USA). The dishes with dye-loaded cells were mounted on the stage of Nikon TMS-F fluorescence inverted microscope with a Cohu 4915 CCD camera. Fluorescent images were captured alternatively at excitation wavelengths of 340 and 380 nm and an emission wavelength of 520 nm. $[\text{Ca}^{2+}]_i$ was calculated by using a ratio equation as described previously.¹⁶

Total RNA extraction

A total cellular RNA isolation kit (Ambion, Austin, TX, USA) was used to extract total RNA from cells according to the manufacturer's instructions.

Quantitative real-time PCR

Adipocyte 18s, UCP2, NADPH oxidase and 11 β -HSD, and muscle UCP3 and NADPH oxidase were quantitatively measured using a Smart Cycler Real-Time PCR System (Cepheid, Sunnyvale, CA, USA) with a TaqMan 1000 Core Reagent Kit (Applied Biosystems, Branchburg, NJ, USA). The primers and probe sets were obtained from Applied Biosystems TaqMan[®] Assays-on-Demand[™] Gene Expression primers and probe set collection according to the manufacturer's instructions. Pooled adipocyte total RNA was serial-diluted in the range of 1.5625–25 ng and used to establish a standard curve; total RNAs for unknown samples were also diluted in this range. Reactions of quantitative RT-PCR for standards and unknown samples were also performed according to the instructions of Smart Cycler System (Cepheid, Sunnyvale, CA, USA) and using the Taqman Real-Time PCR Core Kit (Applied Biosystems, Branchburg, NJ, USA). The mRNA quantitation for each sample was further normalized using the corresponding 18s quantitation.

Determination of intracellular reactive oxygen species generation

Adipose tissue digestion and adipocyte preparation were prepared as described in $[\text{Ca}^{2+}]_i$ measurement. Intracellular ROS generation was assessed using 6-carboxy-2',7'-dichlorodihydrofluorescein diacetate (H2-DCFDA) as described previously.¹⁷ Cells were loaded with H2-DCFDA (2 $\mu\text{mol/l}$) for 30 min before the end of the incubation period (48 h). After washing twice with PBS, cells were scraped and disrupted by sonication on ice (20 s). Fluorescence (emission

543 or 527 nm) and DNA content were then measured as described previously. The intensity of fluorescence was expressed as arbitrary units per ng DNA.

Statistical analysis

Data were evaluated for statistical significance by analysis of variance (ANOVA), and significantly different group means were then separated by the least significant difference test by using SPSS (SPSS Inc. Chicago, IL, USA). All data presented are expressed as mean ± s.e.m.

Results

We first investigated whether aP2-agouti transgenic mice are also a suitable model for the study of diet-induced oxidative stress. Transgenic mice exhibited significantly greater baseline ROS production compared with wild-type controls before the feeding period, and the consumption of the obesity-promoting diet significantly increased adipose tissue ROS production only in aP2-agouti transgenic mice (Figure 1a). This effect was also associated with increased NADPH oxidase expression in adipose tissue of aP2-agouti transgenic mice before and following consumption of the obesity-promoting diet (Figure 1b).

We then utilized aP2 transgenic mice as a model to investigate the effect of dietary calcium on diet-induced oxidative stress in a 3-week study utilizing obesity-promoting (high-sucrose/high-fat) diets with either low calcium (0.4% from CaCO₃) (basal diet) or high calcium

(1.2% from CaCO₃) (high-calcium diet) content. Although feeding high-fat/high-sucrose diets *ad libitum* for 3 weeks induced weight and fat gain in all animals, mice on the high-calcium diet gained only 50% of the body weight ($P=0.04$) and fat ($P<0.001$) of mice on the basal diet (Figure 2). Visceral body fat was disproportionately affected, with the sum of two visceral fat pad weights decreasing from 2.48 ± 0.19 g on the low-calcium diet to 1.31 ± 0.11 g on the high-calcium diet ($P<0.002$); when expressed as a percentage of body weight, the sum of the visceral fat pads decreased from 7.4 ± 0.4 to $4.5 \pm 0.3\%$ ($P<0.001$). There were no significant differences in daily food intakes between the low-calcium diet group and the high-calcium diet group (4.86 versus 4.77 g/day, $P>0.05$). The high-calcium diet also suppressed diet-induced hyperglycemia and reduced fasting blood glucose by 15% compared to mice on the basal diet ($P=0.003$) (Figure 3). The high-calcium diet significantly reduced adipose intracellular ROS production by 64 and 18% ($P<0.001$) in visceral and subcutaneous adipose tissue (Figure 4a). Consistent with this, the high-calcium diet also inhibited adipose tissue NADPH oxidase expression, by 49% ($P=0.012$) in visceral adipose tissue and by 63% ($P=0.05$) in subcutaneous adipose tissue, respectively (Figure 4b). Moreover, adipocyte intracellular calcium ($[Ca^{2+}]_i$) levels, which were previously demonstrated to favor adipocyte ROS production, were markedly suppressed in mice on the high-calcium diet by 73–80% ($P<0.001$) versus mice on the

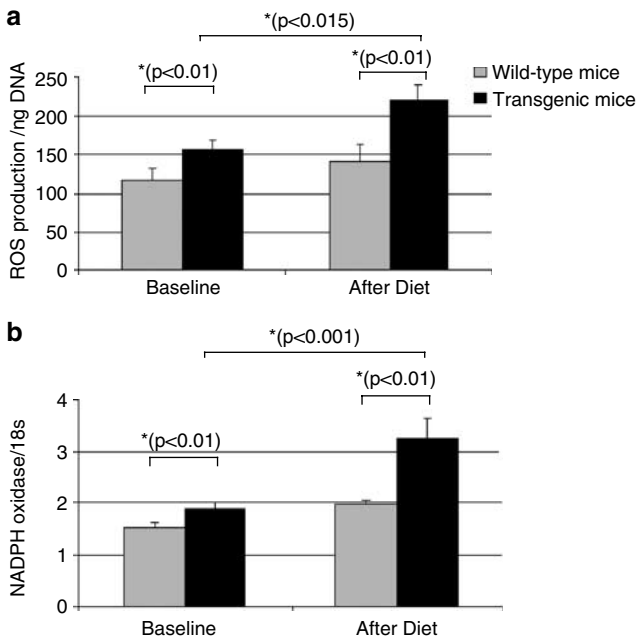


Figure 1 Adipose intracellular reactive oxygen species production (a) and NADPH oxidase expression (b) in wild-type and aP2-agouti transgenic mice. Values are presented as mean ± s.e.m., $n=6$.

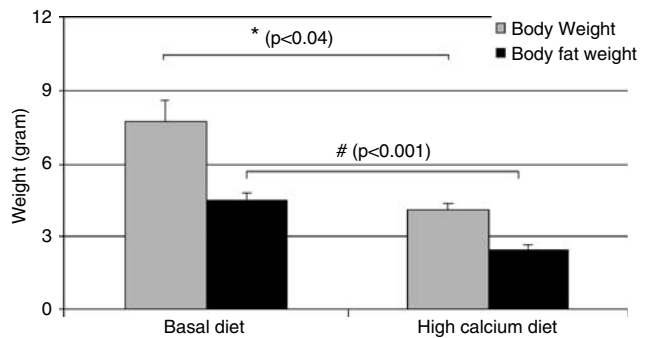


Figure 2 Effect of dietary calcium on body weight and fat pads weight in aP2-agouti transgenic mice. Values are presented as mean ± s.e.m., $n=10$.

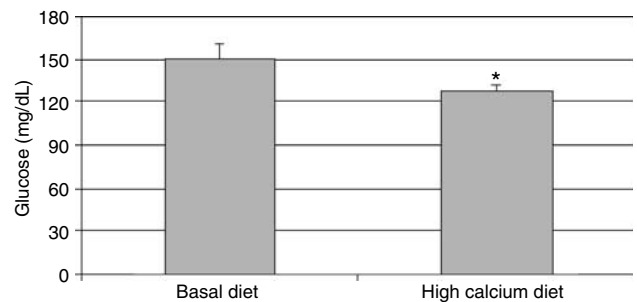


Figure 3 Effect of dietary calcium on fasting blood glucose in aP2-agouti transgenic mice. Values are presented as mean ± s.e.m., $n=10$. *Significant difference from the basal diet, $P<0.05$.

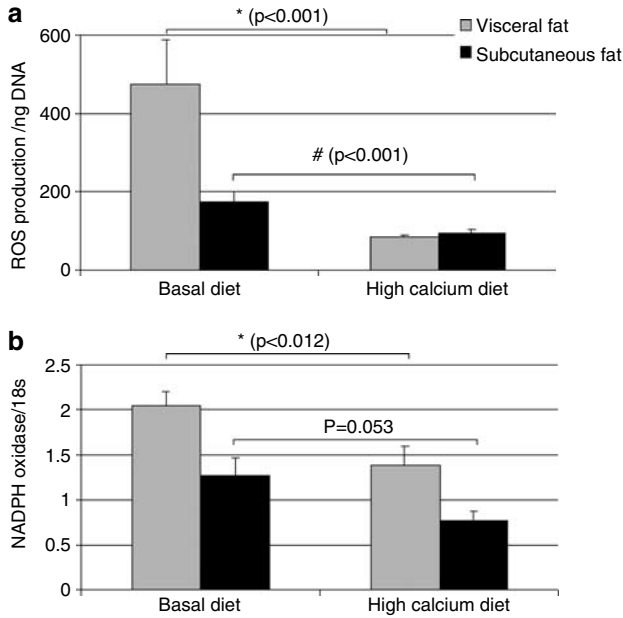


Figure 4 Effect of dietary calcium on adipose intracellular reactive oxygen species production (a) and NADPH oxidase expression (b) in aP2-agouti transgenic mice. Values are presented as mean \pm s.e.m., $n = 10$.

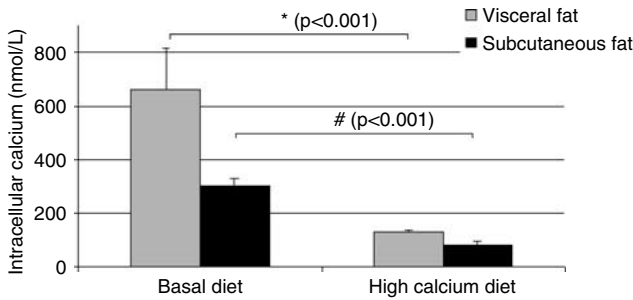


Figure 5 Effect of dietary calcium on adipose intracellular calcium ($[Ca^{2+}]_i$) in aP2-agouti transgenic mice. Values are presented as mean \pm s.e.m., $n = 10$.

basal diet (Figure 5). Consistent with our previous study,⁹ the high-calcium diet also induced 367 and 191% increases in adipose UCP2 expression ($P < 0.001$) in visceral and subcutaneous adipose tissue, respectively, compared to mice on the basal diet (Figure 6a). Moreover, the pattern of UCP3 expression and indices of ROS production in skeletal muscle was consistent with these findings. UCP3 expression was 22% higher ($P = 0.006$) (Figure 6b) and NADPH oxidase expression was 36% lower ($P = 0.001$) (Figure 7) in soleus muscle of mice on the high-calcium diet compared to mice on the low-calcium diet.

The high-calcium diet suppressed 11 β -HSD expression in visceral adipose tissue by 39% ($P = 0.034$) compared to mice on a basal diet (Figure 8). Interestingly, 11 β -HSD expression in visceral fat was markedly higher than in subcutaneous fat in mice on basal low-calcium diet ($P = 0.034$), whereas no difference was observed between the fat depots in mice on the high-calcium diet.

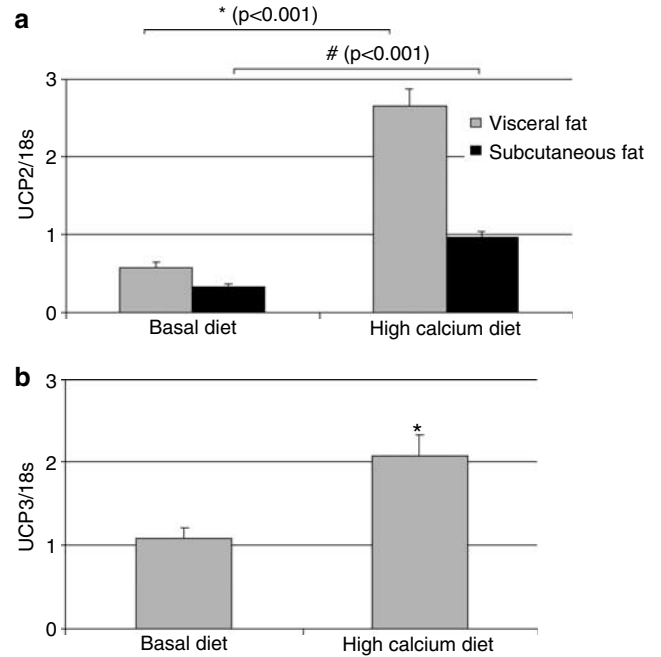


Figure 6 Effect of dietary calcium on adipose UCP2 expression (a) and soleus muscle UCP3 expression (b) in aP2-agouti transgenic mice. Values are presented as mean \pm s.e.m., $n = 10$. *Significant difference from the basal diet, $P < 0.05$.

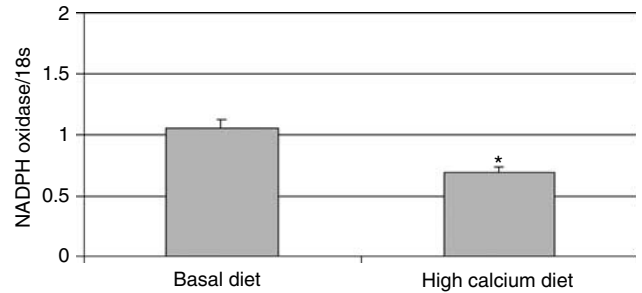


Figure 7 Effect of dietary calcium on soleus muscle NADPH oxidase in aP2-agouti transgenic mice. Values are presented as mean \pm s.e.m., $n = 10$. *Significant difference from the basal diet, $P < 0.05$.

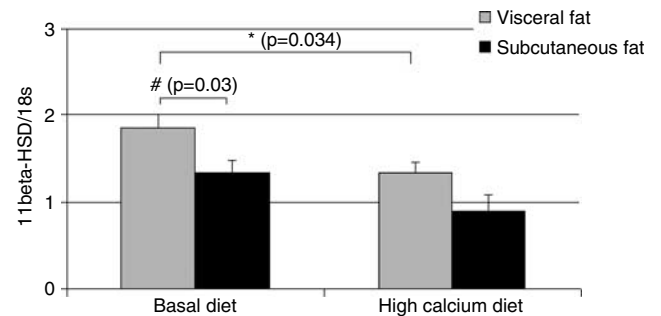


Figure 8 Effect of dietary calcium on adipose 11 β -hydroxysteroid dehydrogenase expression in aP2-agouti transgenic mice. Values are presented as mean \pm s.e.m., $n = 10$.

Discussion

Data from the present study demonstrate that dietary calcium decreased diet-induced ROS production. Previous data from our laboratory demonstrate that dietary calcium exerts an anti-obesity effect via a $1\alpha, 25\text{-(OH)}_2\text{-D}_3$ -mediated mechanism.⁸ We have reported that $1\alpha, 25\text{-(OH)}_2\text{-D}_3$ plays a direct role in the modulation of adipocyte Ca^{2+} signaling, resulting in an increased lipogenesis and decreased lipolysis.^{18,19} In addition, $1\alpha, 25\text{-(OH)}_2\text{-D}_3$ also plays a role in regulating human adipocyte UCP2 expression, suggesting that the suppression of $1\alpha, 25\text{-(OH)}_2\text{-D}_3$ and the resulting upregulation of UCP2 may contribute to increased rates of energy utilization.^{10,11} Accordingly, the suppression of $1\alpha, 25\text{-(OH)}_2\text{-D}_3$ by increasing dietary calcium attenuates adipocyte triglyceride accumulation and caused a net reduction in fat mass in both mice and humans in the absence of caloric restriction,¹³ a marked augmentation of body weight and fat loss during energy restriction in both mice and humans,^{13,20} and a reduction in the rate of weight and fat regain following energy restriction in mice.¹⁴ Our previous data demonstrate that $1\alpha, 25\text{(OH)}_2\text{D}_3$ stimulates Ca^{2+} signaling and suppresses UCP2 expression on human and murine adipocytes^{11,14} and suppresses UCP3 expression in skeletal muscle in mice;¹⁴ accordingly, dietary calcium suppression of ROS production is likely due to suppression of circulating $1\alpha, 25\text{(OH)}_2\text{D}_3$ levels and resultant reductions in Ca^{2+} signaling and increases in UCP2 and UCP3 expression. Furthermore, dietary calcium also appeared to regulate cytosol enzymatic ROS production by inhibiting NADPH oxidase expression, which also contributes to cellular ROS production.

The interaction between ROS and calcium has been intensively investigated.^{21–24} Calcium signaling is essential for production of ROS, and elevated intracellular calcium ($[\text{Ca}^{2+}]_i$) activates ROS-generating enzymes, such as NADPH oxidase and myeloperoxidase, as well as the formation of free radicals by the mitochondrial respiratory chain.²⁵ Interestingly, increased ROS production also stimulates $[\text{Ca}^{2+}]_i$ by activating calcium channels on both the plasma membrane and endoplasmic reticulum (ER).²⁶ Thus, there is a bidirectional interaction wherein ROS regulates cellular calcium signaling, whereas while manipulation of calcium signaling may also regulate cellular ROS production. Consistent with this concept, the present data show that suppression $[\text{Ca}^{2+}]_i$ by high dietary calcium was associated with reduced ROS production in adipose tissue.

Respiration is associated with production of ROS, and mitochondria produce a large fraction of the total ROS made in cells.²⁷ Mild uncoupling of respiration diminishes mitochondrial ROS formation by dissipating mitochondrial proton gradient and potential.²³ Korshunov *et al.*²⁸ have demonstrated that slight increase of the H^+ backflux (to the matrix), which diminishes $\Delta\psi$, results in a substantial decrease in mitochondrial ROS formation. Accordingly, the H^+ backflow induced by uncoupling via UCPs would be expected to down regulate ROS production. Mild activation

of UCPs may therefore play a role in the anti-oxidant defense system and it is reasonable to propose that dietary calcium-induced suppression of $1\alpha, 25\text{-(OH)}_2\text{D}_3$, which has been demonstrated to inhibit UCP2 expression,¹¹ may inhibit ROS production. Indeed, in the present study, we have shown that high dietary calcium up regulated UCP2 expression in adipose tissue and UCP3 expression in skeletal muscle, and these findings were associated with decreased ROS production, indicating a role of mitochondrial uncoupling in the regulation of oxidative stress.

We also compared the ROS production between subcutaneous and visceral adipose tissue. Consistent with our previous data,^{8,29} animals on the basal low-calcium diet showed markedly higher visceral fat gain than subcutaneous fat versus mice on the high-calcium diet and exhibited enhanced ROS production and NADPH oxidase expression in visceral fat versus subcutaneous fat. Conversely, high dietary calcium attenuated visceral fat gain, and mice on the high-calcium diet exhibited similar ROS production in visceral and subcutaneous fat. These results indicate that higher visceral fat predisposes to enhanced ROS production. Accordingly, we further evaluated the involvement of autocrine glucocorticoids by measuring 11 β -hydroxysteroid dehydrogenase (11 β -HSD) expression, the key enzyme responsible for converting glucocorticoid into its active form.³⁰ 11 β -HSD expression in visceral fat was markedly higher than in subcutaneous fat in mice on the basal low-calcium diet, whereas no difference was observed between the fat depots in mice on the high-calcium diet. We also found that the high-calcium diet suppressed 11 β -HSD expression in visceral adipose tissue compared to mice on the low-calcium diet. These findings demonstrate that dietary calcium exerts a greater effect on inhibition of visceral fat gain via suppressing active glucocorticoid production and may therefore explain the markedly decreased visceral fat gain in mice on the high-calcium diet compared with mice on the low-calcium diet. Therefore, the enhanced ROS production observed in visceral fat compared to subcutaneous fat only in mice on a low-calcium diet suggests that suppression of ROS production by dietary calcium may be mediated, in part, by the regulation of glucocorticoid-associated fat distribution. We recently reported that $1\alpha, 25\text{ (OH)}_2\text{D}_3$ directly regulates adipocyte 11 β -HSD 1 expression and local cortisol levels in cultured human adipocytes³¹ by increasing both 11 β -HSD 1 expression and cortisol release. Accordingly, suppression of $1\alpha, 25\text{ (OH)}_2\text{D}_3$ via increasing dietary calcium may inhibit cortisol production in adipose tissue. Data from this study provide the first *in vivo* evidence that dietary calcium inhibits adipose tissue 11 β -HSD expression and may thereby contribute to the preferential loss of visceral adiposity by regulating adipose tissue glucocorticoid production. Moreover, this decrease in visceral adiposity appears to contribute to reduced ROS production.

In conclusion, data from the present study support a role for dietary calcium in the regulation of diet- and obesity-

induced oxidative stress. Potential mechanisms include increases in UCP2 and UCP3 expression, suppression of $[Ca^{2+}]_i$, and/or inhibition of NADPH oxidase and 11 β -HSD gene expression. These data also support our previous observation that dietary calcium inhibits obesity, with partially selective effects on visceral adipose tissue, and leads to significant changes in adipose tissue metabolism, including accelerated adipose tissue accretion and reduced ROS production.

Acknowledgements

This research was supported by an unrestricted grant from The National Dairy Council.

References

- 1 Furukawa S, Fujita T, Shimabukuro M, Iwaki M, Yamada Y, Nakajima Y *et al*. Increased oxidative stress in obesity and its impact on metabolic syndrome. *J Clin Invest* 2004; **114**: 1752–1761.
- 2 Atabek ME, Vatansav H, Erkul I. Oxidative stress in childhood obesity. *J Pediatr Endocrinol Metab* 2004; **17**: 1063–1068.
- 3 Lin TK, Chen SD, Wang PW, Wei YH, Lee CF, Chen TL *et al*. Increased oxidative damage with altered antioxidative status in type 2 diabetic patients harboring the 16189 T to C variant of mitochondrial DNA. *Ann NY Acad Sci* 2005; **1042**: 64–69.
- 4 Sonta T, Inoguchi T, Tsubouchi H, Sekiguchi N, Kobayashi K, Matsumoto S *et al*. Evidence for contribution of vascular NAD(P)H oxidase to increased oxidative stress in animal models of diabetes and obesity. *Free Radic Biol Med* 2004; **37**: 115–123.
- 5 Inoguchi T, Li P, Umeda F, Yu HY, Kakimoto M, Imamura M, Aoki T *et al*. High glucose level and free fatty acid stimulate reactive oxygen species production through protein kinase C-dependent activation of NADPH oxidase in cultured vascular cells. *Diabetes* 2000; **49**: 1939–1945.
- 6 Shangari N, O'Brien PJ. The cytotoxic mechanism of glyoxal involves oxidative stress. *Biochem Pharmacol* 2004; **68**: 1433–1442.
- 7 Chung SS, Ho EC, Lam KS, Chung SK. Contribution of polyol pathway to diabetes-induced oxidative stress. *J Am Soc Nephrol* 2003; **14**: S233–S236.
- 8 Zemel MB. Calcium and dairy modulation of obesity risk. *Obes Res* 2005; **13**: 192–193.
- 9 Sun X, Zemel MB. Role of uncoupling protein 2 (UCP2) expression and 1 α , 25-dihydroxyvitamin D₃ in modulating adipocyte apoptosis. *FASEB J* 2004; **18**: 1430–1432.
- 10 Shi H, Norman AW, Okamura WH, Sen A, Zemel MB. 1 α , 25-Dihydroxyvitamin D₃ modulates human adipocyte metabolism via nongenomic action. *FASEB J* 2001; **15**: 2751–2753.
- 11 Shi H, Norman AW, Okamura WH, Sen A, Zemel MB. 1 α , 25-dihydroxyvitamin D₃ inhibits uncoupling protein 2 expression in human adipocytes. *FASEB J* 2002; **16**: 1808–1810.
- 12 Sun XC, Morris K, Zemel MB. 1, 25(OH)₂D₃ and reactive oxygen species interactively stimulate angiotensinogen expression in differentiated 3T3-L1 adipocytes. *FASEB J* 2005; **19**: A70 (abstract).
- 13 Zemel MB, Shi H, Greer B, Dirienzo D, Zemel PC. Regulation of adiposity by dietary calcium. *FASEB J* 2000; **14**: 1132–1138.
- 14 Sun XC, Zemel MB. Calcium and dairy products inhibit weight and fat regain during *ad libitum* consumption following energy restriction in Ap2-agouti transgenic mice. *J Nutr* 2004; **134**: 3054–3060.
- 15 Reeves PG. Components of the AIN-93 diets as improvements in the AIN-76A diet. *J Nutr* 1997; **127**: 838S–841S.
- 16 Zemel MB. Effects of mitochondrial uncoupling on adipocyte intracellular Ca²⁺ and lipid metabolism. *J Nutr Biochem* 2003; **14**: 219–226.
- 17 Manea A, Constantinescu E, Popov D, Raicu M. Changes in oxidative balance in rat pericytes exposed to diabetic conditions. *J Cell Mol Med* 2004; **8**: 117–126.
- 18 Xue B, Zemel MB. Relationship between human adipose tissue agouti and fatty acid synthase (FAS). *J Nutr* 2000; **130**: 2478–2481.
- 19 Xue B, Moustaid N, Wilkison WO, Zemel MB. The agouti gene product inhibits lipolysis in human adipocytes via a Ca²⁺-dependent mechanism. *FASEB J* 1998; **12**: 1391–1396.
- 20 Zemel MB. Role of calcium and dairy products in energy partitioning and weight management. *Am J Clin Nutr* 2004; **79**: 907S–912S.
- 21 Toescu EC. Hypoxia sensing and pathways of cytosolic Ca²⁺ increases. *Cell Calcium* 2004; **36**: 187–199.
- 22 Ermak G, Davies KJ. Calcium and oxidative stress: from cell signaling to cell death. *Mol Immunol* 2002; **38**: 713–721.
- 23 Miwa S, Brand MD. Mitochondrial matrix reactive oxygen species production is very sensitive to mild uncoupling. *Biochem Soc Trans* 2003; **31**: 1300–1301.
- 24 Brookes PS. Mitochondrial H(+) leak and ROS generation: an odd couple. *Free Radic Biol Med* 2005; **38**: 12–23.
- 25 Gordeeva AV, Zvyagilskaya RA, Labas YA. Cross-talk between reactive oxygen species and calcium in living cells. *Biochemistry (Moscow)* 2003; **68**: 1077–1080.
- 26 Volk T, Hensel M, Kox WJ. Transient Ca²⁺ changes in endothelial cells induced by low doses of reactive oxygen species: role of hydrogen peroxide. *Mol Cell Biochem* 1997; **171**: 11–21.
- 27 Brand MD, Buckingham JA, Esteves TC, Green K, Lambert AJ, Miwa S *et al*. Mitochondrial superoxide and aging: uncoupling-protein activity and superoxide production. *Biochem Soc Symp* 2004; **71**: 203–213.
- 28 Korshunov SS, Skulachev VP, Starkov AA. High protonic potential actuates a mechanism of production of reactive oxygen species in mitochondria. *FEBS Lett* 1997; **416**: 15–18.
- 29 Zemel MB, Richards J, Mathis S, Milstead A, Gebhardt L, Silva E. Dairy augmentation of total and central fat loss in obese subjects. *Int J Obes Relat Metab Disord* 2005; **29**: 391–397.
- 30 Agarwal AK. Cortisol metabolism and visceral obesity: role of 11 β -hydroxysteroid dehydrogenase type I enzyme and reduced co-factor NADPH. *Endocr Res* 2003; **29**: 411–418.
- 31 Morris KL, Zemel MB. 1,25-Dihydroxyvitamin D₃ modulation of adipocyte glucocorticoid function. *Obes Res* 2005; **13**: 670–677.